

Alma Mater Studiorum Università di Bologna
Archivio istituzionale della ricerca

Easy recovery of Li-ion cathode powders by the use of water-processable binders

This is the final peer-reviewed author's accepted manuscript (postprint) of the following publication:

Published Version:

Brilloni, A., Poli, F., Spina, G.E., Samorì, C., Guidi, E., Gualandi, C., et al. (2022). Easy recovery of Li-ion cathode powders by the use of water-processable binders. ELECTROCHIMICA ACTA, 418, 140376-140386 [10.1016/j.electacta.2022.140376].

Availability:

This version is available at: <https://hdl.handle.net/11585/882831> since: 2022-04-21

Published:

DOI: <http://doi.org/10.1016/j.electacta.2022.140376>

Terms of use:

Some rights reserved. The terms and conditions for the reuse of this version of the manuscript are specified in the publishing policy. For all terms of use and more information see the publisher's website.

This item was downloaded from IRIS Università di Bologna (<https://cris.unibo.it/>).
When citing, please refer to the published version.

(Article begins on next page)

This is the final peer-reviewed accepted manuscript of:

A. Brilloni, F. Poli, G. E. Spina, C. Samorì, E. Guidi, C. Gualandi, M. Maisuradze, M. Giorgetti, F. Soavi, Easy recovery of Li-ion cathode powders by the use of water-processable binders, *Electrochim. Acta*, 418 (2022)

The final published version is available online at:
<https://doi.org/10.1016/j.electacta.2022.140376>

Rights / License:

The terms and conditions for the reuse of this version of the manuscript are specified in the publishing policy. For all terms of use and more information see the publisher's website.

This item was downloaded from IRIS Università di Bologna (<https://cris.unibo.it/>)

When citing, please refer to the published version.

Easy recovery of Li-ion cathode powders by the use of water-processable binders

Alessandro Brilloni¹, Federico Poli¹, Giovanni Emanuele Spina¹, Chiara Samorì¹, Elena Guidi¹, Chiara Gualandi¹, Mariam Maisuradze², Marco Giorgetti^{2,3}, Francesca Soavi^{1,3}*

¹Department of Chemistry “Giacomo Ciamician”, Alma Mater Studiorum Università di Bologna, Via Selmi 2, 40126 Bologna (Italy)

²Department of Industrial Chemistry “Toso Montanari”, Alma Mater Studiorum Università di Bologna, Via del Risorgimento 4, 40136 Bologna (Italy)

³National Reference Center for Electrochemical Energy Storage (GISEL) - INSTM, Via G. Giusti 9, 50121 Firenze (Italy)

Abstract

The continuous growth of the lithium batteries market calls for strategies that simultaneously target high energy/power system performance, sustainable manufacturing processes, exploitation of green raw materials and easy recycling of batteries. Here we propose the use of pullulan, a water-soluble and biodegradable polymer, as a binder for the production of LIB cathodes based on $\text{Li}(\text{Ni}_{0.5}\text{Mn}_{0.3}\text{Co}_{0.2})\text{O}_2$ (NMC532). We aim to contribute to the development of a sustainable LIB

value chain, where devices are designed in view of the recovery of critical elements at their end-of-life. In fact, the aqueous manufacturing of the cathodes represents a green, cheap and easy procedure to produce electrodes with reduced environmental impact and recover Li-ion cathode powders from spent LIBs. The cathodes exhibited up to 135 mAh g⁻¹ of composite material and 167 mAh g⁻¹ of NMC, and excellent cycling stability over 500 cycles along with good capacity retention at high C-rates. NMC and carbon black were directly recovered by dissolving the binder through a water-fed aerograph in less than 2 minutes. Notably, the waste waters used to wash and recover the NMC-carbon powders were biodegradable, which is of great importance to close the “sustainability chain” loop.

Keywords: water-processable cathodes, NMC, lithium battery, recycling, pullulan.

1. Introduction

Lithium-ion batteries (LIBs) are considered one of the main enabling technologies within the European Green Deal roadmap [1,2]. In fact, LIBs are even more irrupting into e-mobility and energy storage from intermittent renewable energy sources. In this scenario, strategies that simultaneously target high energy/power performance, sustainable manufacturing processes, valorisation of green raw materials and easy recycling of LIBs are urgently needed [3, 4].

As it concerns LIB manufacturing, the transition towards the use of low cobalt content cathodes, like Li(Ni_xMn_yCo_z)O₂ (NMC), is considered a good option. It features a specific capacity that can be higher than 160 mAh/g (depending on the Ni:Mn:Co stoichiometry) and a working potential higher than 4 V vs Li⁺/Li [4, 5]. In addition, to meet the requirements of sustainable and cheaper

production processes, much effort is being devoted to the substitution of F-based components with alternative ones. Indeed, today the commonly used binders are F-based polymers, like poly(vinylidene difluoride) (PVdF) which needs N-methyl-2-pyrrolidone (NMP) as solvent/dispersant, both very toxic for humans and the environment. Europe has included NMP in the list of substances of very high concern and has recently set severe limits on its use [6]. Today, the use of PVdF for electrode processing requires expensive atmosphere-controlled environments and has a great economic and environmental impact on LIBs manufacturing [7-9]. Furthermore, the presence of F-containing polymers might generate volatile and toxic fluorocarbons during the traditional incineration of spent LIBs [7].

Transition to aqueous electrode preparation by non-toxic binders is expected to provide a great step forward towards an ideally sustainable and environmentally friendly technology for energy storage systems. Furthermore, the low environmental impact during the manufacturing and end-of-life management of aqueous binders open a new approach towards the design for recycling of LIBs [7-13]. Natural polymers, like cellulose, alginate, guar gum have already been reported as viable alternatives to PVdF [7-17].

Pullulan (PU) is an exopolysaccharide produced from starch by *Aureobasidium pullulans*. It is based on linked maltotriose repeating units that confer high film- and fiber-forming characteristics to pullulan. Pullulan films exhibit excellent mechanical properties, are edible, biodegradable, O₂-impermeable, resistant in an alkaline environment, and highly water-soluble. For these characteristics, pullulan is attracting much attention for pharmaceutical and biomedical applications and, more recently as a component (binder and/or separator) of electrochemical energy storage devices, like supercapacitors and high-voltage LNMO LIBs [19, 20]. Specifically, pullulan:glycerol with 1:1 mixtures (PUGLY) were used for their excellent binding properties.

Indeed, glycerol acts as a plasticizer and improves the mechanical properties of the polymer film [20, 21]. Pullulan was also reported as a component of binder formulations for silicon anodes of LIBs [22]. Beside cell manufacturing, LIB component recycling is also a key topic that has to be addressed to fulfill the system sustainability challenge. The increasingly growing LIB market brings about an increasing demand for lithium and cobalt, with the consequent price increase and related concerns about the future and long-term material availability [23-25].

End-of-life LIBs are managed by three main approaches: rebuild, retrofit and recycle. Recycling is the best option. It enables the inclusion of exhausted LIBs within a circular economy approach, considering them as resources rather than waste to be disposed of. Hence, used or exhausted batteries can be considered as a huge reserve of raw material, reusable for the construction of new LIBs [23-27].

Critical metals from exhausted LIB electrodes can be recovered by pyrometallurgical, hydrometallurgical, electrochemical methods that can be also combined [28]. The first step is the mechanical separation of LIB components that usually takes place by breaking or shredding off electrodes. Alternatively, it is possible to separate the current collector sheets from the composite material through thermal processes that degrade the binder at 150-500 °C or pyrolysis [28]. In such processes, however, HF can develop due to the degradation of the electrolyte. Direct recycling by the dissolution of the PVdF binder through the use of NMP, γ -butyrolactone, dimethylformamide or dimethyl sulfoxide is a valuable alternative. However, even in this case, toxic solvents that require controlled work environments are required [24, 26, 28]. Cathodes manufactured with water-soluble binders can be directly recycled to recover the black mass (active cathode powder and carbon additive) by physical separation from metal current collectors through a simple immersion in water and avoiding any harmful organic solvent, which dramatically reduces the

recycling environmental impact and cost. This approach has been successfully demonstrated for $\text{Li}(\text{Ni}_{0.5}\text{Mn}_{0.3}\text{Co}_{0.2})\text{O}_2$ (NMC532) cathodes processed by several binders like carboxymethyl cellulose (CMC), styrene-butadiene rubber (SBR), and PVdF latex NMC532 powders that were recollected by sonication, washing and sintering at 700°C [9].

It is worth noting that failure in manufacturing of LIBs, i.e. electrode cutting (for pouch cells) or cell assembly errors, could impact on the total manufacturing costs by ca. 26%, which may lead to the loss material during the manufacturing process, causing to lowering the yield to 75%. Direct and easy recycling of scraps electrodes produced by aqueous binders could decrease the overall manufacturing costs by reintroducing valuable active materials in the manufacturing stream [9-11].

Here we propose the use of the water-soluble and biodegradable polymer pullulan (PU) to manufacture NMC532 cathodes (hereafter labelled with PUGLY-NMC). PU allows a green, cheap and easy procedure to produce electrodes and recover Li-ion cathode powders from spent LIBs. Indeed, black mass was directly recovered by dissolving the binder through a water-fed aerograph, without any additional sintering step. The PUGLY-NMC production and direct recycling concept is depicted in Figure 1.

The electrochemical performance of PUGLY-NMC electrodes tested in cells with Li-metal anodes is reported and compared to that of cathodes featuring PVdF. Electrochemical tests are complemented with structural and morphological analyses of fresh, aged cathodes and recovered powders (from production wastes). In addition, the aerobic and anaerobic biodegradability of the PUGLY and PVdF binders is evaluated to demonstrate the possibility of managing the waste waters used to wash and recover the NMC-carbon powders from the PUGLY-NMC electrodes through conventional biological treatments. Hence, overall, this paper aims at demonstrating that

PU-processed electrodes can be viewed as LIB components “designed in view of recycling” and manufactured in compliance with the green chemistry principles [29]. Indeed, LIB cathode manufacturing by water-based processes in the ambient atmosphere, as well as the easy NMC powder recovery (from aged cells and/or cathode production wastes), enable to address the principles “1. Prevention”, “3 Less Hazardous synthesis”, “4. Design Safer Chemicals”, “5. Use of Renewable Feedstocks”, “6. Reduce derivatives” and “7. Inherently Safer Chemistry for Accident Prevention”.

2. Experimental

2.1. PUGLY-NMC cathode preparation

PUGLY-NMC cathodes were produced using a commercial NMC532 powder (Shandong Gelon Lib.Co) with stoichiometry $\text{Li}(\text{Ni}_{0.5}\text{Mn}_{0.3}\text{Co}_{0.2})\text{O}_2$ (see EDS data in the Supplementary Information section, Figure S1) and particle size 9-12 micron [30].

Electrodes were produced by casting NMC-based composites on aluminum current collectors (20 μm -thick). Before casting, aluminum foils were treated to remove passivation layers. Specifically, the foils were immersed in a 5% wt KOH aqueous solution for 1 minute, washed with milliQ water and dried in an oven overnight at 80°C.

NMC and carbon conductive additive (SuperC45, Imerys Graphyte Carbon), with a mass ratio 89.47:10.53 were dry-milled at 250 rpm over 30 minutes by a planetary ball mill (FRITSCH, Pulverisette) using tungsten jar (12 mL) and spheres (10 spheres, 5 mm diameter). This step enabled a good dispersion of the carbon particles within the oxide grains.

Then, the aqueous solution of pullulan (binder, TCI Europe, Zwijndrecht, Belgium) and glycerol (plasticizer, Sigma-Aldrich) with 1:1 mass ratio and 40% w/w_{total} of milliQ was added in the jar, to obtain a slurry that was milled at 250 rpm over 20 minutes. The slurry milling time and the amount of water were kept as small as possible in order to minimize side reactions between NMC and water. In fact, it has been reported that exchange $\text{Li}^+ \rightleftharpoons \text{H}^+$ reactions can take place during immersion of NMC cathode powders in water [31]. In turns this might bring about the formation of LiOH and to the increase of pH. Such increase could favour the formation of Li_2CO_3 , by the reaction with CO_2 from the atmosphere, and promote aluminum corrosion during the casting procedure [13, 17]. The pH of the slurry was checked and resulted in 10.67 ± 0.02 . The pH of the PUGLY solution, without NMC and carbon was 6.7 ± 0.02 . To avoid a prolonged contamination with the atmosphere, PUGLY-NMC layers were casted immediately after slurry milling on pre-etched aluminum foils. The final composition of the PUGLY-NMC cathodes was: 85% NMC, 10% carbon conductive additive, 5% PUGLY. The composite slurry was casted on the aluminum foil by a Mini Coating Machine (Hohsen Corporation) at 0.3 cm s^{-1} and with a bar distance of $200 \mu\text{m}$. The coated films were dried at 60°C overnight in a thermostatic oven, pressed at 4 Ton/cm^2 , and dried again under dynamic vacuum (BUCHI oven) at 120°C overnight to eliminate any trace of water. Finally they were transferred in a dry box under Argon atmosphere (MBraun, H_2O and $\text{O}_2 < 1 \text{ ppm}$).

Cathodes featuring PVdF binder were produced by a similar approach that is detailed in Supplementary Information.

2.2. Chemical-physical analyses

The morphological characterization of the materials was carried out using a Zeiss EVO 50 electron scanning microscope (SEM) equipped with an energy-dispersive X-ray analyzer (EDS) from Oxford INCA Energy 350 system. Low magnification images of bent cathodes were collected by a Skybasic digital microscope (1000X). X-ray diffraction (XRD) spectra were collected by a PANalytical X'Pert PRO powder diffractometer equipped with a X'Celerator detector (CuK α radiation, $\lambda = 1.5406 \text{ \AA}$, 40 mA, 40 kV), radiation source and Ni filter by continuous scanning mode (step 0.017° 2θ step size, 10 s/step scan rate). The reported XRD patterns have been corrected for the background and, in the case of the electrodes, for a 0.3 mm displacement of the XR beam focal plane.

Thermogravimetric Analysis (TGA) was performed by a TA Thermal Analysis Q50 equipment, under Argon/O₂ flow (60 mL/min) with a scan rate of $10^\circ\text{C}/\text{min}$ up to 650°C . Dynamic Mechanical Analysis (DMA) were performed with a dynamic mechanical analyzer DMA Q800 TA Instrument on rectangular samples in tensile mode and under strain control. The storage (E') and loss modulus (E'') were monitored for 10 min while applying a strain amplitude of 0.06% at an oscillation frequency of 1 Hz.

2.3. Electrochemical tests

PUGLY-NMC electrodes (0.9 cm diameter) were tested in 2-electrode Swagelock cells in Teflon with AISI 316L connectors. Lithium metal was used as the negative electrode. Before the use, lithium was mechanically treated and laminated to remove any passivation layer. The separator

used to assemble the cell was a Celgard (2300, 25 μm -thick) film. The electrolyte used was 1 M LiPF_6 in 1:1 (w:w) ethylene carbonate (EC):dimethyl carbonate (DMC) (LP30, Selectlyte BASF, Germany). The cells were assembled in a dry box. The electrochemical measurements were carried out at 30°C by a multi-channel VMP (Perkin Elmer, Waltham, MA, USA) potentiostat/galvanostat.

At first, PUGLY-NMC cathodes were subjected to a conditioning protocol that consisted in voltammetric (CV) and galvanostatic charge/discharge cycles that were carried out with a charge cut-off voltage of 4.2 V vs. Li^+/Li . Afterwards, electrochemical tests were performed increasing the charge cut-off at 4.5 V vs. Li^+/Li . For the galvanostatic tests, the C-rate was calculated on the basis of the nominal specific capacity provided by the NMC provider, i.e. 150 mAh g^{-1} [30].

2.4. NMC-carbon recovering and biodegradation studies

The NMC-carbon recovery process was tested on large PUGLY-NMC foils (area of 56 cm^2) that were not cycled. to get quantitative data. The average areal mass loading of the composite layer was $6 \pm 1 \text{ mg cm}^{-2}$. The films were weighed and then the PUGLY-NMC composite was collected by dissolving the PUGLY binder with water spray by an aerograph fed with compressed air. The obtained aqueous suspension containing dissolved PUGLY and the NMC-carbon black mass was filtered by a syringe filter (Millex-GV Millipore Coop., 0.22 μm) that was also used to wash with hot water the powder trapped in the filter. The filter with the black mass was removed from the filter holder, dried at 120 °C in a thermostatic oven. Finally, the NMC-carbon composite was collected from the filter.

To evaluate the biodegradability of the waste-waters used to wash and recover the NMC-carbon powders from the electrodes, aerobic and anaerobic tests were carried out on aqueous solutions of

PUGLY and PVdF. Aerobic biodegradation was determined by a ready biodegradability test in an aqueous medium according to the OECD (Organization for Economic Cooperation and Development) guideline 301 F, “Manometric respirometry”, using an activated sludge taken from a treatment plant receiving domestic sewage located in Ravenna, Italy, as the bacterial inoculum [32]. The anaerobic degradation was performed at 55°C for 15 days by using a mix of anaerobically-digested sewage sludge from local waste-water treatment plants of different agro-food industries, and following the procedure reported in ref. [33] (the amount of biogas produced was evaluated by visual quantification of the volume produced every day, while the percentage of methane was determined by analysing 10 mL of the biogas through a GC-TCD, Agilent 78120A).

2.5 X-ray absorption spectroscopy measurements

X-ray absorption spectroscopy (XAS) experiments at the Ni, Mn and Co K-edges were performed at Elettra Sincrotrone Trieste (Italy), at the XAFS 11.1 beamline [34]. The storage ring operated at 2.4 GeV in top-up mode with a typical current of 160 mA. Data were recorded in transmission mode using ionization chambers filled with a mixture of Ar, N₂, and He to have 10, 70, and 95% of absorption in the I0, I1, and I2 chambers, respectively. An internal reference of nickel, manganese and cobalt foil was used for energy calibration. The white beam was monochromatized using a fixed exit monochromator equipped with a pair of Si (111) crystals. Spectra were collected with a constant k-step of 0.03 Å⁻¹ with 2 s per point acquisition time from 6345 to 7090 eV, from 7515 to 8320 eV, and from 8155 to 8820 eV around Mn, Co and Ni K-edges, respectively.

3. Results

3.1. PUGLY-NMC cathode production

PUGLY-NMC cathodes were obtained following the steps described in Section 2.1 and in Figure

1.

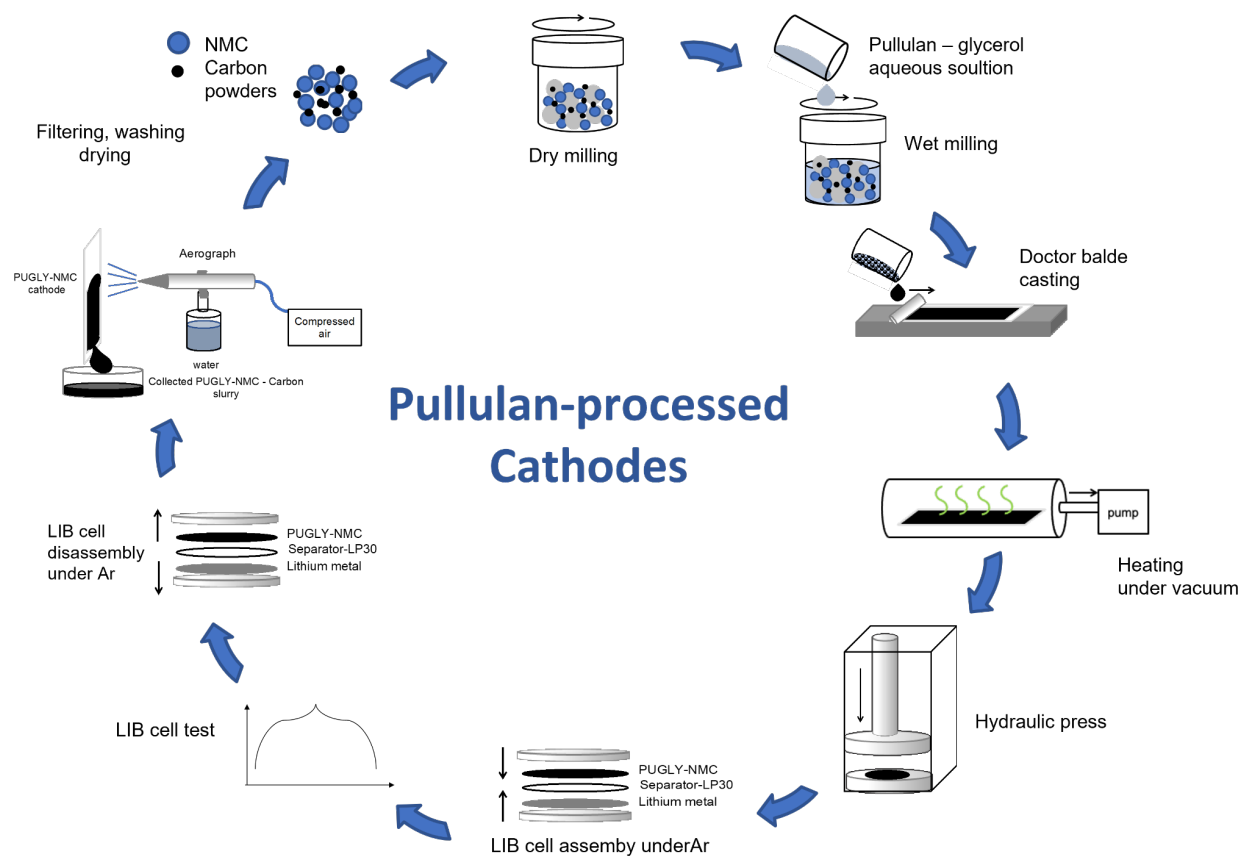


Figure 1. PUGLY-NMC cathode production process and schematic of the entire direct recycling process. In this paper, direct recycling was demonstrated on fresh-prepared cathodes (not cycled).

Figure 2 and Figure 3 report the SEM image and XRD pattern of the pristine NMC powder and PUGLY-NMC cathodes. The comparison of Figures 2a and 2b suggests that the ball milling step is beneficial to get a homogeneous dispersion of carbon and binder among the NMC grains, and to reduce the size of the largest NMC agglomerates ($> 10 \mu\text{m}$). In addition, no significant difference was observed in the XRD spectra after the water processing-(see also XRD reflection positions in Table S1). All the patterns display a single-phase $\alpha\text{-NaFeO}_2$ -type structure [35]. No additional reflections that could be ascribed to contaminants like LiOH or Li_2CO_3 were observed in the X-ray patterns. The split of the (006)/(102) and (108)/(110) doublets indicates a good hexagonal ordering that is representative of the layered structure, and that was kept before and after electrode processing [34, 35]. Table 1 reports lattice parameters a and c refined by the rhombohedral system with R-3m space group, as well as the ratio of the integrated intensities of the (003) and (104) reflections (I_{003}/I_{104}), that is taken as an indicator of cation mixing, i.e. the partial occupation of Ni^{2+} lattice sites by Li^+ . High (I_{003}/I_{104}) indicates small $\text{Li}^+/\text{Ni}^{2+}$ cation mixing [36]. For the pristine NMC532 powder, the a and c parameters are 2.87 Å and 14.21 Å, and the I_{003}/I_{104} ratio is 0.93. Table 1 reports the Ni, Mn and Co atomic ratio evaluated by SEM-EDS that confirmed the NMC532 stoichiometry. Both XRD parameters and EDS results obtained for the pristine NMC532 powder are similar to those evaluated for the PUGLY-NMC electrode, therefore suggesting that the bulk lattice of NMC was well maintained after electrode processing by PUGLY. This conclusion was further supported by XAS analyses, discussed in Section 3.4, that indicated that the pristine NMC bulk chemical and structural environment of Mn, Co, and Ni was retained in PUGLY-NMC electrodes.

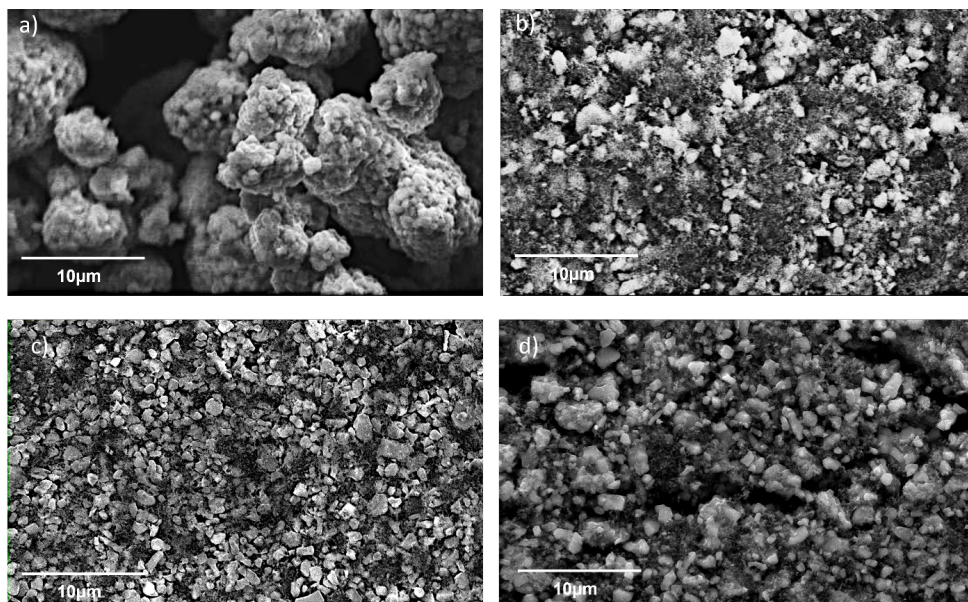


Figure 2. SEM images of a) pristine NMC powder, b) pristine PUGLY-NMC electrode, c) PUGLY-NMC electrode after 500 galvanostatic cycles, and d) recovered black mass

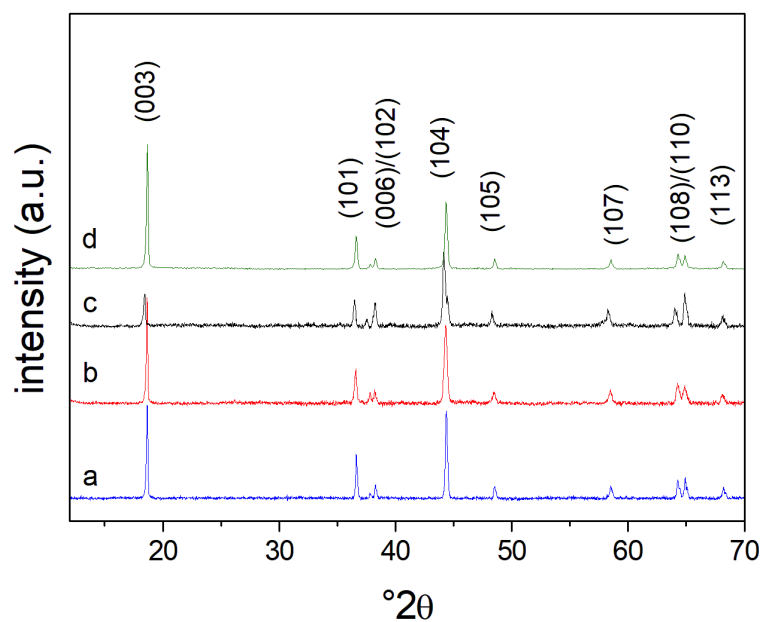


Figure 3. XRD patterns of a) pristine NMC powder, b) pristine PUGLY-NMC electrode, c) PUGLY-NMC electrode after 500 galvanostatic cycles, d) NMC-carbon powder recovered from waste cathode (not cycled).

Table 1. Lattice parameters a , c , ratios of the integrated intensities of the (003) and (104) reflections (I_{003}/I_{104}), and EDS stoichiometric ratio of Ni, Mn and Co.

Sample	XRD			EDS atomic ratio		
	a (Å)	c (Å)	I_{003}/I_{104}	Ni	Mn	Co
Pristine NMC powder	2.87	14.21	0.96	4.9	3.1	2.0
Fresh PUGLYNMC electrode	2.86	14.19	0.93	4.8	3.0	2.0
Cycled PUGLYNMC electrode	2.85	14.16	0.33	4.8	3.1	2.0
Recovered NMC-carbon powder	2.87	14.17	1.10*	4.7	2.9	2.0

**averaged over several spectra*

The average mass loading of the PUGLY-NMC coating was evaluated by weighing different samples cut as disks (0.9 cm diameter) from the main aluminum coated strip (Figure 4a). Up to $6 \pm 1 \text{ mg cm}^{-2}$ of composite layer and 4.8 mg cm^{-2} of NMC was deposited on Al. The layer was well stuck on the current collector and no cracks were observable even at a millimetric magnification (Figure 4b).

Electrode manufacturing upscale by automatic roll machine requires that high bending flexibility and resistance to elongation are achieved without damaging the composite material coating. In addition, for cost- and time-effective electrode production, high temperatures are often used to dry electrodes [37]. We tested the flexibility of the PUGLY-NMC cathode strips (9 cm width and c.a. 15 cm long) by wrapping them around a 5 cm diameter steel cylinder. Figure 4c-d reports the images of the flexibility study and show that the PUGLY-NMC cathodes exhibited excellent mechanical properties, with no crack formation after the test.

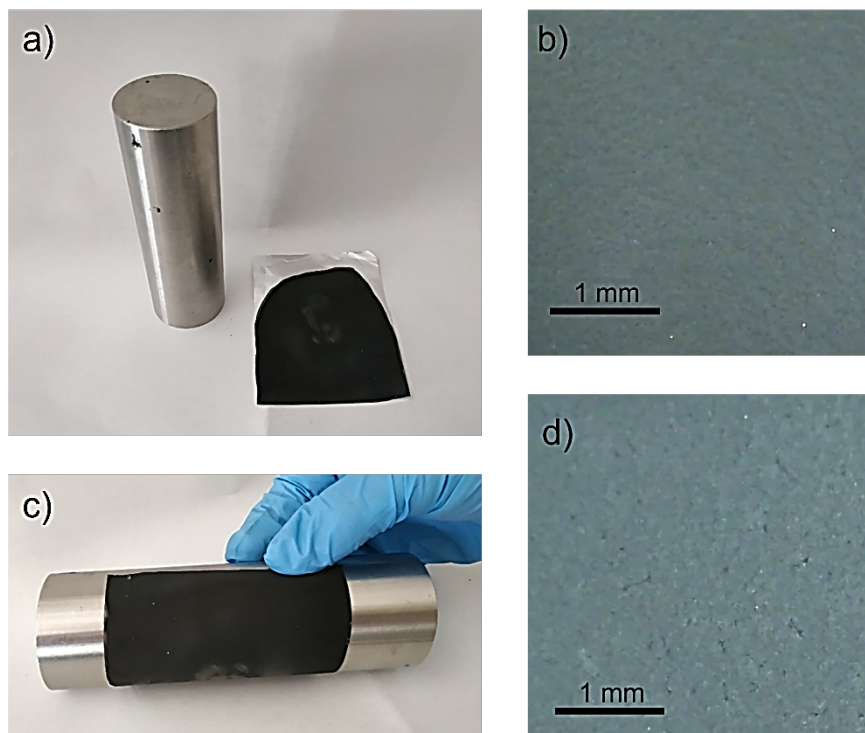


Figure 4. a) PUGLY-NMC coated aluminum strip, b) magnification of the coating layer, c) flexibility test, d) magnification of the coating layer during flexibility test.

Electrode integrity was also evaluated during a DMA analysis where small deformations were applied to the electrode for a prolonged time. The measurements were carried out to compare the behavior of PU based and PVdF based electrodes under the same test condition. The measurements were performed under controlled strain at room temperature by applying an oscillating strain of $\varepsilon = 0.06\%$ for 10 minutes. The application of a higher strain of 0.08% resulted in the break of the aluminum current collector. Figure 5 shows that both storage modulus and loss modulus did not change during the DMA test, meaning that both electrodes maintained their mechanical properties without being damaged under the investigated conditions.

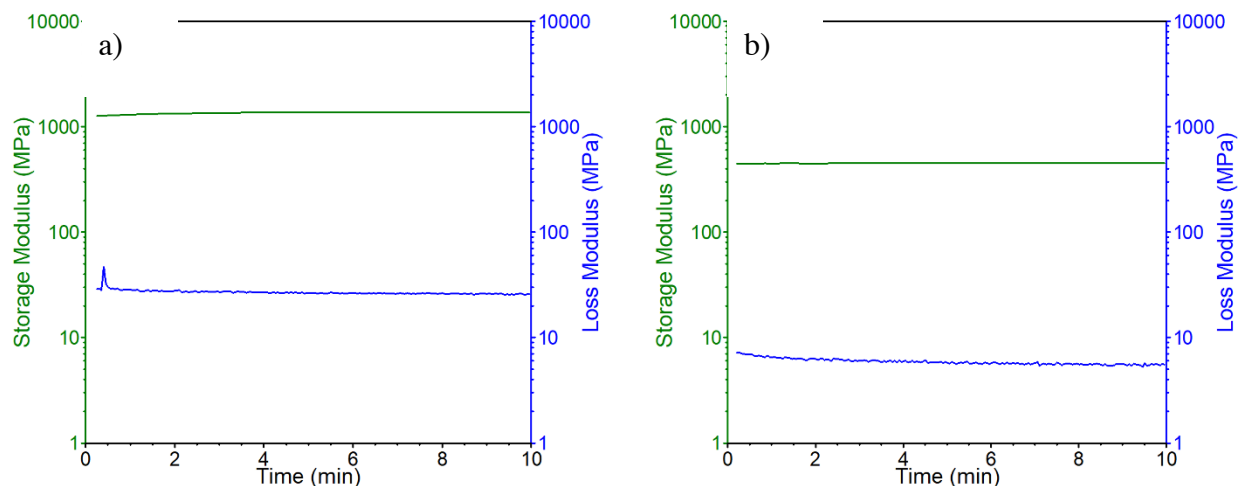


Figure 5. DMA measurements under controlled strain at RT by applying a 0.06% strain of a) PU electrode and b) PVdF electrode

Figure 6 shows the TGA profiles under Ar/O₂ of the milled black mass (NMC and carbon, without binder) and of a PUGLY-NMC cathode (the aluminum mass has been excluded). In absence of binder, i.e. in the case of the black mass sample, the mass loss between 270°C and 300°C can be attributed to surface carbonates formed after exposure to water and air [38]. Oxygen evolution from the NMC lattice at these temperatures can be appreciated only in delithiated samples [39] (for a comparison, see also the TGA analysis of the pristine NMC powder without carbon, Figure S3). This loss partially overlaps with the binder degradation, as evidenced by the comparison of the curve of the black powder and of the PUGLY-NMC cathode. Indeed, pullulan is known to exhibit a high thermal stability at temperatures even up to 200°C in an inert atmosphere [40, 41]. The mass loss before 200°C of the cathode (black line) can be attributed to the PUGLY binder that under oxygen atmosphere loses 50% of its weight as shown in Figure S3. The additional

10% mass loss between 450 and 500°C is related to the combustion of the carbonaceous component.

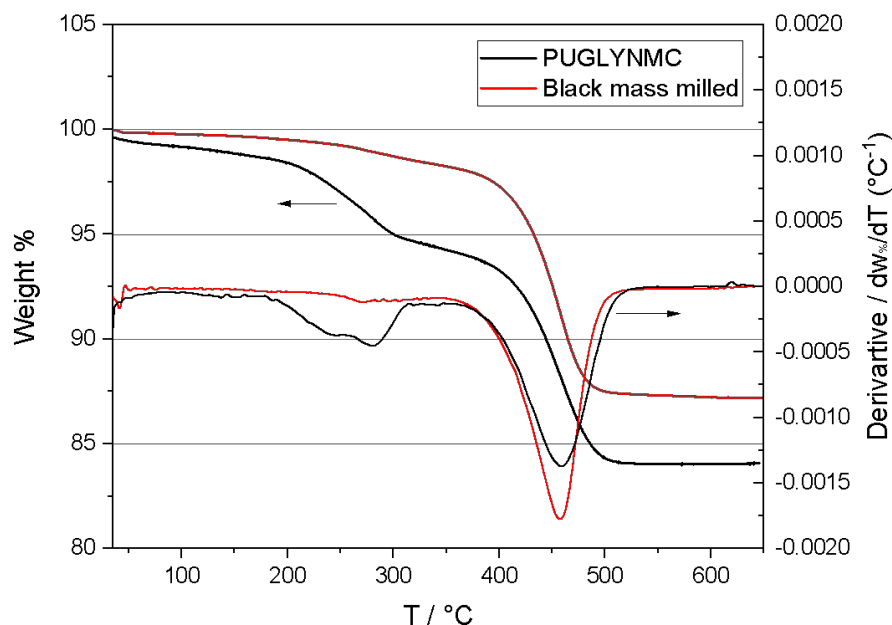


Figure 6. TGA profiles under Ar/O₂ and their derivatives of the milled black mass (NMC and carbon, red line), and of the pristine PUGLY-NMC cathode (the aluminum mass has been excluded, black line).

3.2. PUGLY-NMC cathode electrochemical test

At first, the electrodes were cycled in a narrow electrode potential window, i.e. between 2.5 V and 4.2 V vs Li⁺/Li in Li/LP30/NMC cells. Figure 7 compares the results of the voltammetric and galvanostatic tests run in this potential range of PUGLY-NMC and PVdF -NMC electrodes featuring the same mass loading (ca. 5.5 mg cm⁻²). Specifically, the following test protocol was adopted: 5 CVs at 20 μV/s, galvanostatic cycles at C/10, C/5, C/3, C/1 and C/5 (both for charge

and discharge), and 3 CVs at $20 \mu\text{V/s}$. Figure 7a compares the CVs of the two electrodes before and after the galvanostatic cycles at C/10. For both PUGLY-NMC and PVdF-NMC, galvanostatic cycling improved electrode response. Indeed, for PUGLY-NMC, the voltammetric capacity increased from $103 \text{ mAh g}_{\text{NMC}}^{-1}$ to $121 \text{ mAh g}_{\text{NMC}}^{-1}$. For the PVdF-NMC it changed from $106 \text{ mAh g}_{\text{NMC}}^{-1}$ to $125 \text{ mAh g}_{\text{NMC}}^{-1}$. This behavior could be explained with the improvement of electrode wettability by the electrolyte promoted by cycling. After this sort of activation, the CVs of PUGLY-NMC and PVdF-NMC overlapped. Figures 7b and Figure S4 show that even under galvanostatic test, the two electrodes feature similar behavior. Also, the capacity retention of the electrodes was similar. Indeed, when the C/rate increased from C/10 to 1C, the specific capacity of PVdF-NMC decreased from $115 \text{ mAh g}_{\text{NMC}}^{-1}$ to $99 \text{ mAh g}_{\text{NMC}}^{-1}$. For PUGLY-NMC, specific capacity correspondingly decreased from $115 \text{ mAh g}_{\text{NMC}}^{-1}$ to $96 \text{ mAh g}_{\text{NMC}}^{-1}$.

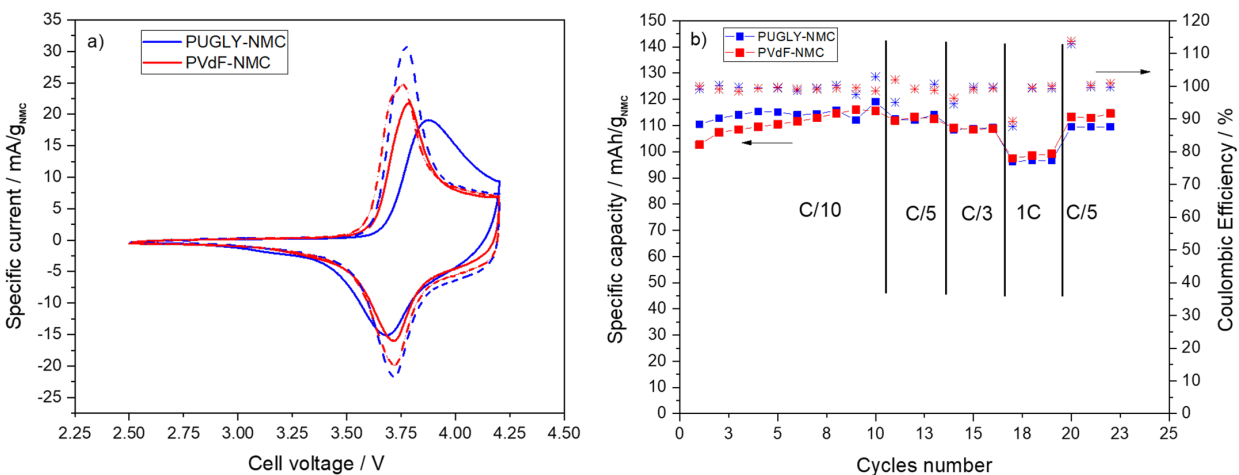


Figure 7. a) Cyclic voltammograms at $20 \mu\text{Vs}^{-1}$ before (solid lines) and after (dashed lines) the galvanostatic tests, and b) trends of the specific capacity (squares) and coulombic efficiency (asterisks) under the rate capability tests at C/5, C/3 and 1C of Li/LP30/NMC cells with PUGLY-

NMC or PVdF electrodes (ca. 5.5 mg cm⁻²) with cell cut-off voltages 2.5 V - 4.2 V. Specific current and capacity values are calculated on the content of NMC.

After the first conditioning cycles, the PUGLY-NMC cathode was further tested in a wider electrode potential range, by setting the charge cut-off voltage at 4.5 V. Figure 8a reports the trend of the cycled capacity and coulombic efficiency over 500 cycles carried out at C/3 and 1C. The 1C rate was considered an accelerated aging test condition. The cell featured an outstanding cycle stability. Only after 450 cycles, 200 of each carried out at 1C, the capacity started to slightly fade. Worth noting, we used an as received lithium metal anode and no SEI forming additives were present in the electrolyte. Therefore, the observed fading could be ascribed not only to the cathode, but also to the lithium anode operation. Periodically, C-rate capability tests with charge/discharge at C/5, C/3, 1C and C/5 (4 cycles for each C-rate) were run as a diagnostic tool to check the cell state-of-health. As an example, Figure 8b reports the capacity and coulombic efficiency trends during one of the C-rate capability tests. Figure 8c shows representative galvanostatic profiles at different C-rates of the cell. The PUGLY-NMC cathodes featured 165 mAh g⁻¹, 153 mAh g⁻¹, 147 mAh g⁻¹, 126 mAh g⁻¹, and 85 mAh g⁻¹, when calculated taking into account just the NMC content. Therefore, the electrochemical tests indicated that PUGLY can be considered as a valuable green alternative to PVdF. Indeed, the nominal performance of the NMC cathode powder, as for the manufacturer, is > 150 mAh g⁻¹ [30]. After the full electrochemical characterization, after 500 cycles, the Li/LP30/PUGLY-NMC was disassembled in a dry box and the PUGLY-NMC recovered and washed with acetonitrile. The electrode was analyzed by SEM-EDS and XRD and the results are reported in Figures 2c and 3c, and in Table 1. The comparison with the data collected with the pristine PUGLY-NMC cathodes highlights that the material did not undergo significant structural and morphological changes after cycling. However, after cycling, I₀₀₃/I₁₀₄ decreased

from 0.93 to 0.33, hence suggesting Ni and Li ions interchange with each other's sites in the crystal lattice.

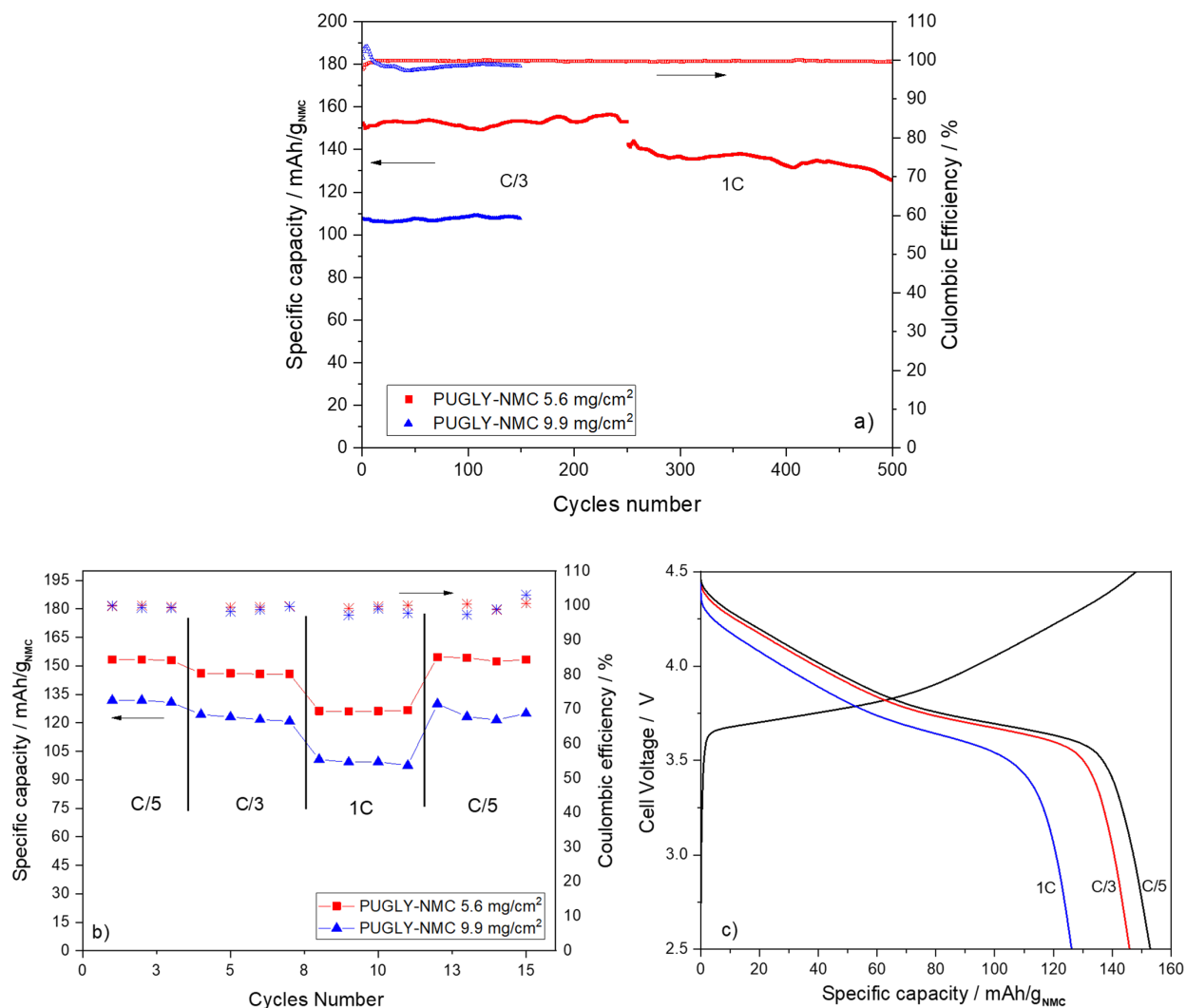


Figure 8. Galvanostatic tests of the Li/LP30/PUGLY-NMC (5.6 mg cm⁻²) cell at 4.5 V cut-off potential: trends of the specific capacity and coulombic efficiency a) over repeated cycles at C/3 and C/1, and b) under the rate capability tests at C/5, C/3, 1C, c) galvanostatic profiles for selected C-rates. Specific capacity values are calculated on the content of NMC. Figures a) and b) include the capacity trend over cycling of a thicker electrode featuring 9.9 mg cm⁻² of PUGLY-NMC.

In order to approach practical conditions, the mass loading of PUGLY-NMC electrodes was doubled. Figure 8a and 8b include the results of the galvanostatic cycling tests for an electrode featuring 9.9 mg cm^{-2} of PUGLY-NMC. The increase of the mass loading brings about the decrease of the cycled capacity, presumably because of a lack of optimized ionic and electronic connections of NMC particles. However, it is worth noting that PUGLY enables good mechanical and electrochemical stability even at higher mass loadings. Indeed, the thicker electrode kept 100% of its initial capacity over 150 cycles.

3.3. PUGLY-NMC electrode direct recycling

An easy method to recover NMC from composite electrodes was set up. The cycled electrodes featured only 0.9 cm diameter and, hence, few mg of PUGLY-NMC, which is too low to quantitatively demonstrate the recycling process and to recover enough material for further analysis. Therefore, the direct recycling method was demonstrated using large PUGLY-NMC cathode films casted on aluminum, freshly prepared (not cycled). Specifically, in the first step, the films were weighed and then the PUGLY-NMC composite was collected by dissolving the PUGLY binder with water spray by an aerograph fed with compressed air. Second step is the water filtering of the composite powder, which was performed with a syringe and a disc filter by firstly pumping the water resulting from the first step and later with demineralized water. Figure 9 shows procedure and that PUGLY-NMC easily detached from the aluminum layer in a few seconds.

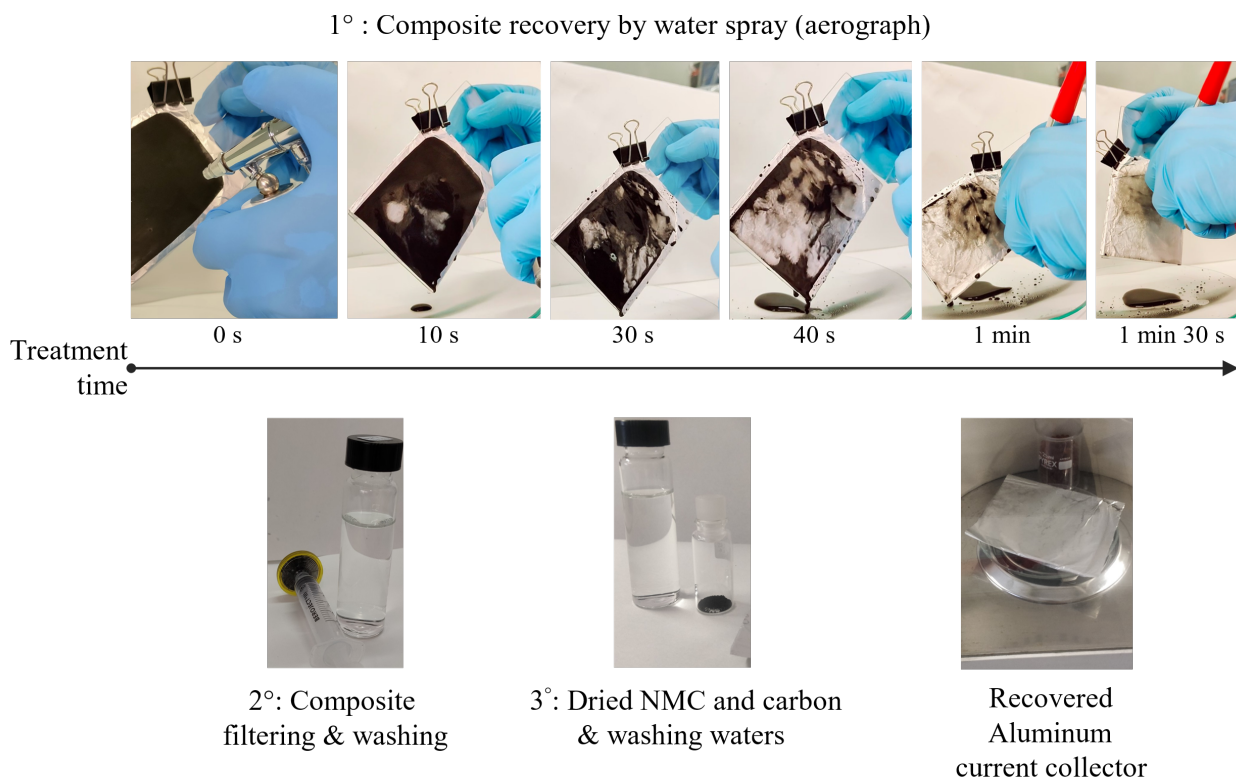


Figure 9. Procedure to recover PUGLY-NMC composite from casted electrodes by water-spray divided in three steps.

Finally, the biodegradability of the PUGLY solution obtained after the recovery of the binder from the electrode was tested and compared to that of PVdF, both under aerobic and anaerobic conditions (Figure 10). Under aerobic conditions, PUGLY reached 34% of biodegradation in 50 days, while a complete biodegradation was achieved in just 15 days under anaerobic conditions. As expected, PVdF was highly persistent under both the aerobic and anaerobic conditions tested (0-2% of biodegradation observed in 50-60 days). These results demonstrate the environmental potential of binders like PUGLY if compared to the conventional PVdF binder, indicating these bio-based binders enable the design of a manufacturing-to recycling electrode process where the binder impact is completely reduced.

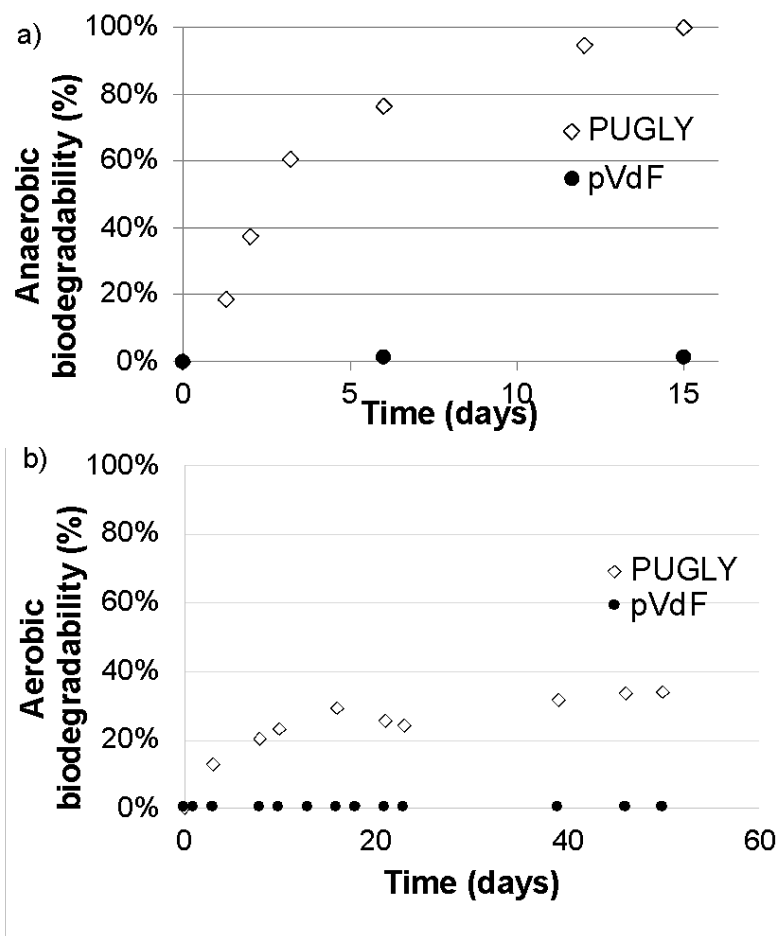


Figure 10. Biodegradability of PUGLY and PVdF binders under (a) anaerobic and (b) aerobic conditions.

The collected powder was filtered and washed with water and finally dried at 120 °C overnight. The powder, shown in Figure 9, consists of an NMC-carbon composite.

XRD, EDS, and XAS analyses (Figure 3, Table 1 and Section 3.4) indicated that the crystalline domain of the NMC active material is retained. In fact, XRD NMC patterns of the recovered powder overlap those of the pristine one.

Given that delithiated NMC tends to release oxygen above 250 °C [39], and that carbon burns above 400 °C (Figure 6), direct recycling of the black composite can be a viable approach to keep the pristine chemical and structural features of the active material. Therefore, the NMC-carbon

mixture can be reused to produce new PUGLY-NMC electrodes, closing the recycling loop, as demonstrated by Figure 11 that compares the first CVs of thick PUGLY-NMC electrodes assembled with the fresh NMC powder and the recovered black mass. The voltammograms of the two electrodes are comparable, suggesting that the electrochemical behavior of NMC is preserved after the recovery process. The specific capacity of the recovered electrode is $76 \text{ mAh g}_{\text{NMC}}^{-1}$, lower than that of the fresh one ($95 \text{ mAh g}_{\text{NMC}}^{-1}$), but this difference has to be mainly explained with the high loading of the former electrode (15.6 mg cm^{-2}) vs. the latter (9.9 mg cm^{-2}) and with the fact that it was not galvanostatically activated.

In any case to restore NMC degradation, a process of revitalization, i.e. correction of the lithium stoichiometry, could be performed. Many approaches have been proposed, like NM reconditioning through conventional solid-state reactions by adding external Li sources (e.g., carbonate or sulfate) [42]. NMC treatment with concentrated Li-ion solutions, through hydrothermal process and subsequent heating steps regenerated the lattice and electrochemical features of NMC with limited cost ($< 10 \$ \text{ Kg}$) [43]. As it concerns pullulan, we consider it as a waste that being biodegradable does not need to be recovered, as well as further purification of waste waters is not needed. In any case to recover PU, Heating and Solvent Precipitation steps can be performed, following the procedure already proposed for its fermentative production [44].

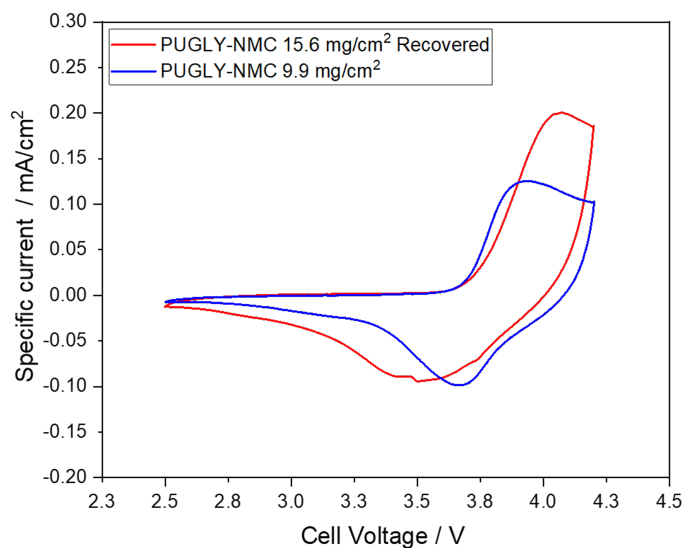


Figure 11. Comparison of the CVs at $20 \mu\text{Vs}^{-1}$ of a fresh PUGLY-NMC electrode (9.9 mg cm^{-2}) and of an electrode produced by using the recovered black mass (15.6 mg cm^{-2})

3.4 XAS analyses

To validate the recovery process, an x-ray absorption spectroscopic study has been conducted on the pristine NMC powder, the fresh PUGLY-NMC electrode, and the recovered black powder. The results are presented in Figure 12. By using the strong selectivity of the XAS probe for the atomic species, the local structure and oxidation state changes associated with the manganese, nickel and cobalt can be revealed. As seen from the different panels of the Figure 12, which represent nickel, manganese and cobalt K edges of recovered powder compared to the pristine powder and pristine electrode, the three spectra have a close match for all the three elements, indicating the absence of the structural and chemical modification of the local coordination of those metals during the recovery process. The only difference is slight decrease of edge jump peak intensity of Ni and Mn (very little in case of Co) of PUGLY-NMC electrode, which is

understandable, as additional compounds are present in the electrode formulation, whereas recovered powder spectra follows the spectra of the pristine powder. Furthermore, each set of spectra characterized by a pre-edge peaks, here depicted as A, position of which is indicative of the formal charge and then the oxidation state [45]. Once again, no shift in the energy position of such a feature is detected in the three panels. The absence of any detectable shift in the edge position of the spectra suggests that the local charges associated with Mn, Co and Ni are the same while comparing pristine and the recovered powder. This is also confirmed by the EXAFS data (Figure S5). In all cases two shells are visible: metal (Ni, Mn, or Co respectively) oxygen interaction as the first shell and interaction to metal as the second one: Ni(Mn, Co)-M(Ni, Mn, Co). No local structural changes are visible.

Overall, XAS technique confirmed the same chemical, and structural environment of Mn, Co and Ni in the pristine and recovered powders and electrodes. This fact is striking, also taking into consideration that the XAS probes not only the surface of a sample but also its bulk behavior.

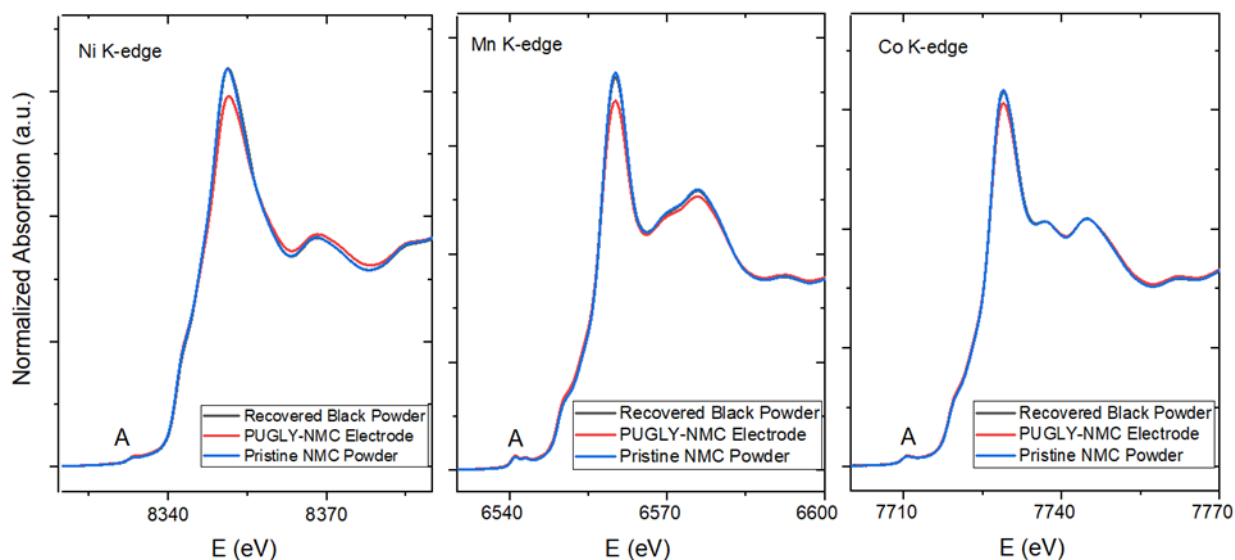


Figure 12. XAS signals of the pristine NMC powder, the fresh PUGLY-NMC electrode, and the recovered NMC-carbon black powder.

4. Conclusions

Overall, our study demonstrates that the use of water-soluble and biodegradable polymer pullulan for the manufacturing of LIB cathodes is a valuable alternative to traditional binders based on fluorine polymer and has a potential to the development of a sustainable LIB value chain, where devices are designed in view of the recovering of critical elements at their end-of-life.

Specifically, the high-potential cathodes PUGLY-NMC, based on NMC532 and pullulan, were produced in the ambient atmosphere, by avoiding the use of toxic solvents and fluorinated binders. Not only the cathodes featured mechanical properties that are suitable for an automatic production by roll-to-roll equipment, but, and mainly, they exhibited excellent cycling stability over 500 cycles along with good capacity retention at high C-rates.

The use of PUGLY binder will, first of all, decrease electrode manufacturing costs. Electrode production cost based solely on the materials, includes the cost of active materials, carbon, and the binder solution used for the slurry. Table S2 (supplementary information) reports the costs of different binder solutions. The evaluation has been done considering the production of composite electrodes featuring 5% binder, by using inks (including powders, binder and solvent) prepared with 40% of solvent (as in this work), i.e. with a binder concentration in the solution of 7.5%. The cost of a binder solution featuring PVdF (8-10 USD kg⁻¹) in NMP (1-3 USD kg⁻¹), can be as high as 3.5 USD kg⁻¹ [7]. For PVdF-based solutions, the major cost comes from NMP. Substitution of NMP with water (0.015 USD kg⁻¹) dramatically decreases the cost of the binder solution. As an example, 7.5 % wt. CMC (2-5 USD kg⁻¹) aqueous solutions, even with the addition of other polymers/plasticisers, like Styrol-Butadien rubber (SBR, 2-3 USD kg⁻¹), will cost lower than 0.36 USD kg⁻¹ [7].

At present PU (20-30 USD kg⁻¹, [46]) is more expensive than CMC, but its mechanical properties are superior [47], as well its increasing market is forecasting a significant cost reduction. However, a solution of 7.5% PUGLY in water, with 1:1 PU:GLY (0.4-0.5 USD kg⁻¹ [48]) ratio, costs only 1,0 USD kg⁻¹. This specific cost is 70% lower than that of the PVdF-NMP solution. Despite being affected by the binder to solvent ratio, and binder content in the composite electrodes, these cost values indicate the potential cost reduction by transitioning to water-based electrodes from the materials' point of view. In addition, it has to be underlined that using the aqueous solution would avoid the need of the environments with controlled atmosphere required for processing NMP, with further advantages in terms of costs. In addition, the use of the water processable binder could enable a green, cheap, fast and easy procedure to recover the Li-ion cathode black powders from the cathodes. Indeed, we directly recovered NMC by dissolving the binder and collecting the powders in less than 2 minutes by means of a water-fed aerograph. The waste-waters used to wash and recover the NMC-carbon powders are biodegradable, which is of great importance to close the “sustainability chain” loop. In addition, NMC active material does not suffer any structural and chemical modifications after the recovery process, as verified by the bulk and atomic sensitive XAS investigation.

The size (0.9 cm diameter) of the cycled electrodes was too low to recover enough material for further analysis. Hence, at present, the recovery process has been demonstrated only by using large PUGLY-NMC cathode films casted on aluminum, freshly prepared (not cycled). Work on the assembly and direct recovery of large pouch cells, that will further strengthen our concept, is planned. In any case, the proposed procedure could pave the way towards a further reduction of LIB manufacturing costs by reducing active material losses related to production errors and

inaccuracies which today account for the 26% of the total manufacturing costs. Indeed, NMC could be easily recovered from production scraps and put back in the main production stream.

Corresponding Author

Francesca Soavi , francesca.soavi@unibo.

Supporting Information: PVdF-NMC cathode preparation process; SEM pictures and EDS spectra of the pristine NMC523 powder, TGA profiles under argon of the pristine NMC powder and PUGLY polymer composite, TGA profile under O₂ of the PU/GLY polymer composite, galvanostatic profiles for selected C-rates of PUGLY-NMC and PVdF-NMC electrodes, and comparison of the k₂-extracted EXAFS signal taken at the Mn, Ni and Co K-edges and their corresponding Fourier Transform, for all investigated electrodes and powders.

Acknowledgments

“Piano Triennale di Realizzazione 2019-2021, Accordo di Programma Ministero dello Sviluppo Economico” – ENEA and “New generation of electrochemical energy storage systems”- Progetto Alte Competenze per la Ricerca e il Trasferimento Tecnologico POR FSE 2014/2020 - REGIONE EMILIA ROMAGNA are acknowledged for the financial support. Measurements at ELETTRA were funded by the Ceric project number 20212162 (M. Giorgetti as PI).

REFERENCES

1. European Commission, The European Green Deal, Brussels, 11.12.2019, COM(2019) 640 final, https://ec.europa.eu/info/strategy/priorities-2019-2024/european-green-deal_en . *Date of access 02/11/2021*
2. Killer, M. , Farrokhseresht, M. , Paterakis, N. G. ; Implementation of large-scale Li-ion battery energy storage systems within the EMEA region, *Applied Energy*, 260 (2020) 114166
3. Dühnen, S., Betz, J., Kolek, M., Schmuck, R., Winter, M., Placke, T. Toward Green Battery Cells: Perspective on Materials and Technologies. *Small Methods* 4 (2020) 2000039.
4. Mauler, L. , Duffner, F. , Leker, J. , Economies of scale in battery cell manufacturing: The impact of material and process innovations, *Applied Energy* 286 (2021) 116499
5. Manthiram, A. A reflection on lithium-ion battery cathode chemistry. *Nat Commun* 11 (2020) 1550.
6. European Commission, Annex XVII to REACH (Regulation concerning the Registration, Evaluation, Authorisation and Restriction of Chemicals, Brussels, 9.4.2019 SWD (2019) 1300 final, <https://eur-lex.europa.eu>. *Date of access 02/11/2021*
7. Bresser, D., Moretti, A., Varzi, A., Passerini, S. Alternative Binders for sustainable electrochemical energy storage—the transition to aqueous electrode processing and bio-derived polymers. *Energy Env. Sci.* 11 (2018) 3096.
8. Wood, D. L., Quass, J. D., Li, J. , Ahmed, S., Ventola, D., Daniel, C. Technical and economic analysis of solvent-based lithium-ion electrode drying with water and NMP. *Dry. Technol.* 36 (2018) 234–244.

9. Li, J., Lu, Y., Yang, T., Ge, D., Wood III, D. L., Li, Z. Water-Based Electrode Manufacturing and Direct Recycling of Lithium-Ion Battery Electrodes—A Green and Sustainable Manufacturing System. *iScience* 23 (2020) 101081.
10. Schröder, R., Aydemir, M.; Seliger, G. Comparatively Assessing Different Shapes of Lithium-ion Battery Cells, *Procedia Manufacturing*, 8 (2017) 104-111
11. Liu, Y., Zhang, R., Wang, J., Wang, Y. Current and future lithium-ion battery manufacturing. *iScience*, 24(2021):102332.
12. Costa, C.M., Lizundia, E., Lanceros-Méndez, S. Polymers for advanced lithium-ion batteries: State of the art and future needs on polymers for the different battery components. *Prog. Energy Combust. Sci.* 79 (2020) 100846
13. Wood, M., Li, J., Ruther, R. E., Du, Z., Self, E. C., Meyer, H. M., Daniel, C., Belharouak, I., Wood, D. L. Chemical stability and long-term cell performance of low-cobalt, Ni-Rich cathodes prepared by aqueous processing for high-energy Li-Ion batteries. *Energy Storage Mater.* 24 (2020) 188-197.
14. Prosini, P. P., Cento, C., Carewska, M., Masci, A. Electrochemical performance of Li-ion batteries assembled with water-processable electrodes. *Solid State Ion.*, 274 (2015) 34-39.
15. Bigoni, F., De Giorgio, F., Soavi, F., Arbizzani, C. Sodium alginate: a water-processable binder in high-voltage cathode formulations. *J. Electrochem. Soc.*, 164 (2016) A6171
16. De Giorgio, F., La Monaca, A., Dinter, A., Frankenberger, M., Pettinger, K.-H., Arbizzani, C. Water-processable $\text{Li}_4\text{Ti}_5\text{O}_{12}$ electrodes featuring eco-friendly sodium alginate binder. *Electrochim. Acta* 289 (2018) 112-119.

17. Kuenzel, M., Bresser, D., Diemant, T., Vieira Carvalho, D., Kim, G.-T., Behm, J., Passerini, S. Complementary Strategies Toward the Aqueous Processing of High-Voltage $\text{LiNi}_{0.5}\text{Mn}_{1.5}\text{O}_4$ Lithium-Ion Cathodes. *ChemSusChem*. 11 (2018) 562–573
18. Poli, F., Momodu, D., Spina, G. E., Terella, A., Mutuma, B. K., Focarete, M. L., Manyala, N., Soavi, F. Pullulan-ionic liquid-based supercapacitor: A novel, smart combination of components for an easy-to-dispose device. *Electrochim. Acta* 338 (2020) 135872
19. Spina, G.E., Poli, F., Brilloni, A., Marchese, D., Soavi, F. Natural polymers for green supercapacitors. *Energies* 13 (2020) 3115-3131.
20. Vuddanda, P.R., Montenegro-Nicolini, M., Morales, J.O., Velaga, S. Effect of plasticizers on the physico-mechanical properties of pullulan based pharmaceutical oral films. *Eur. J. Pharmaceut. Sci.* 96 (2017) 290-298.
21. Tong, Q., Xiao, Q., Lim, L.T. Preparation and properties of pullulan–alginate–carboxymethylcellulose blend films. *Food Res. Int.* 41 (2008) 1007-1014.
22. Preman, A. N., Lee, H., Yoo, J., Kim, I.T., Saito, T., Ahn, S. Progress of 3D network binders in silicon anodes for lithium ion batteries. *J. Mater. Chem. A* 8 (2020) 25548-25570.
23. Zheng, X., Zhu, Z., Lin, X., Zhang, Y., He, Y., Cao, H., Sun, Z. A Mini-Review on Metal Recycling from Spent Lithium Ion Batteries. *Engineering* 4 (2018) 361.
24. Greenwood, M. , Wentker, M. , Leker, J. , A region-specific raw material and lithium-ion battery criticality methodology with an assessment of NMC cathode technology. *Applied Energy* 302 (2021) 117512
25. Fan, E. , Li, L., Wang, Z., Lin, J., Huang, Y., Yao, Y., Chen, R., Wu, F. Sustainable Recycling Technology for Li-Ion Batteries and Beyond: Challenges and Future Prospects. *Chem. Rev.* 120 (2020), 7020.

26. Liu, C., Lin, J., Cao, H., Zhang, Y., Sun, Z. Recycling of spent lithium-ion batteries in view of lithium recovery: A critical review. *J. Clean. Prod.* 228 (2019) 801.
27. Oliveira, L., Messagie, M., Rangaraju, S., Sanfelix, J., Rivas, M., Mierlo, J. Key issues of LIBs from resource depletion to environmental KPI. *J. Clean. Prod.* 108 (2015) 354.
28. Yao, Y., Zhu, M., Zhao, Z., Tong, B., Fan, Y., Hua, Z. Hydrometallurgical Processes for Recycling Spent Lithium-Ion Batteries: A Critical Review. *ACS Sustain. Chem. Eng* 6 (2018) 13611 - 13627
29. <https://www.acs.org/content/acs/en/greenchemistry>. Date of access 02/11/2021
30. <http://www.libgroup.net/index.html>. Date of access 02/11/2021
31. Shkrob, I. A., Gilbert, J. A., Phillips, P. J., Klie, R., Haasch, R. T., Bareño, J., & Abraham, D. P. Chemical weathering of layered Ni-rich oxide electrode materials: evidence for cation exchange. *Journal of The Electrochemical Society.* (2017) 164 A1489.
32. Torri, C., Fabbri, D. Biochar enables anaerobic digestion of aqueous phase from intermediate pyrolysis of biomass. *Biores. Tech.* 172 (2014) 335 - 341
33. Guideline for Testing of Chemicals: Ready Biodegradability; OECD Guideline 301; Organization for Economic Cooperation and Development: Paris, 1992
34. Aquilanti, G., Giorgetti, M., Dominko, R., Stievano, L., Arcon, I., Novello, N. Olivi, L. Operando characterization of batteries using x-ray absorption spectroscopy: advances at the beamline XAFS at synchrotron Elettra. *J. Phys. D. Appl. Phys.* 50 (2017) 074001
35. Li, T., Yuan, X. Z., Zhang, L., Song, D., Shi, K., Bock, C. Degradation Mechanisms and Mitigation Strategies of Nickel-Rich NMC-Based Lithium-Ion Batteries. *Electrochem. Energ. Rev.* 3 (2020) 43–80

36. Zhang, X., Jiang, W.J., Mauger, A., Qilu, Gendron, F., Julien, C.M. Minimization of the cation mixing in $\text{Li}_{1+x}(\text{NMC})_{1-x}\text{O}_2$ as cathode material. *J. Power Sources* 195 (2010) 1292-1301.
37. Ruschhaupt, P., Varzi, A., Passerini, S. Natural Polymers as Green Binders for High-Loading Supercapacitor Electrodes. *Chem. Sus. Chem.* 13 (2020) 763-770.
38. Sicklinger, J., Metzger, M., Beyer, H., Pritzl, D., Gasteiger, H. A. Ambient Storage Derived Surface Contamination of NCM811 and NCM111: Performance Implications and Mitigation Strategies. *J. Electrochem. Soc.* 166 (2019) A2322-A2335
39. Min Bak, S., Hu, E., Zhou, Y., Yu, X., Senanayake, S. D., Cho, S. J., Kim, K.B., Chung, K. Y., Yang, X. Q., Nam, K. W. Structural Changes and Thermal Stability of Charged $\text{LiNi}_x\text{Mn}_y\text{Co}_z\text{O}_2$ Cathode Materials Studied by Combined In Situ Time-Resolved XRD and Mass Spectroscopy. *ACS Appl. Mater. Interfaces* 6 (2014) 22594–22601
40. Gualandi, C., Zucchelli, A., Fernández Osorio, M., Belcari, J., Focarete, M. L. Nanovascularization of Polymer Matrix: Generation of Nanochannels and Nanotubes by Sacrificial Electrospun fibers. *Nano Lett.* 13 (2013) 5385–5390.
41. Strasser, C. How Stable is Pullulan? TGA-FT-IR Provides Fast Answers, *NGB Application note 124*, <https://www.netzsch-thermal-analysis.com>. Date of access 02/11/2021
42. Ferrara, C., Ruffo, R., Quartarone, E. and Mustarelli, P. Circular Economy and the Fate of Lithium Batteries: Second Life and Recycling. *Adv. Energy Sustainability Res.*, 2 (2021) 2100047
43. Sloop, S. E., Crandon, L., Allen, M., Lerner, M. M.; Zhang, H., Sirisaksoontorn, W.; Gaines, L.; Kim, J.; Lee, M. Cathode healing methods for recycling of lithium-ion batteries. *Sustainable Mater. Technol.*, 22 (2019) e00113

44. Krishna, G. V. S. R., Srinivasulu, K., Usha, M., Bodaiah, B., Kumar, Y.V.V., Vijaya, M., Sudhakar, P. Sequential Heating and Solvent Precipitation For Effective Pullulan Recovery From Jaggery Based Fermentation Broths. *Journal of Pharmacy Research*. 10 (2016) 296-300
45. Buchholz, D., Li, J., Passerini, S., Aquilanti, G., Wang, D., Giorgetti, M. X-ray absorption spectroscopy investigation of lithium-rich, cobalt-poor layered-oxide cathode material with high capacity. *ChemElectroChem*. 2 (2015) 85-97
46. Farris, S., Unalan, I. U., Introzzi, L., Fuentes-Alventosa, J. M., Cozzolino, C. A. Pullulan-based films and coatings for food packaging: Present applications, emerging opportunities, and future challenges. *J. Appl. Polym. Sci.* 131 (2014) 40539
47. Preman, A. N.; Lee, H.; Yoo, J.; Kim, I.T.; Saito, T.; Ahn, S. Progress of 3D network binders in silicon anodes for lithium ion batteries. *J. Mater. Chem. A*. 8 (2020) 25548-25570.
48. Abdul Aziz, A. R., Tan Hooi W., Archina, B. Two-Step Purification of Glycerol as a Value Added by Product From the Biodiesel Production Process. *Frontiers in Chemistry* 7 (2019) 2296